PAPER Nr. : 56

TRANSIENT BEHAVIOUR OF A ONE–BLADED HORIZONTAL–AXIS WIND TURBINE

BY

R. WENNEKERS

MESSERSCHMITT–BÖLKOW–BLOHM GMBH
MUNICH, GERMANY

TENTH EUROPEAN ROTORCRAFT FORUM

AUGUST 28 – 31, 1984 – THE HAGUE, THE NETHERLANDS

Abstract

The wind energy converter (WEC) "MONOPTEROS" is a 1:3 model scale test version (tower-height: 50 m) of a single-bladed 5.4 MW horizontal-axis wind turbine. It was developed and designed by Messerschmitt-Bölkow-Blohm Corp., Munich under contract to the Ministry of Research and Technology of the Federal Republic of Germany, and is a realization of a "soft", supercritically operating wind turbine concept. The down-wind positioned see-saw rotor operates within a rotational frequency range of 0.55 - 0.84 Hz, which is above the first tower bending eigenfrequency of 0.46 Hz (design tip speed ratio: $\lambda = 12$, rated wind speed: 10 m/s). Owing to the gimbaled suspension, the rotor is allowed to perform, besides the rotational degree of freedom, a teetering motion within a range of 11,5 deg. "MONOPTEROS" is connected to the grid of the Bremerhaven electricity system and is delivering the designed power of 370 kW during the ongoing tests.

In this contribution, aerodynamic and dynamic modelling techniques, the development of control strategies for the transition into/out of nominal performance as well as simulations and measured time-histories, with emphasis on transient operating conditions, are presented.

The paper concludes that for the prediction of transients, which are the most problematic operating phases of the supercritical, one-bladed wind turbine concept, the modelling of classical, stationary rotor aerodynamics is sufficient, but an exact description of the control system is needed.

Notation

ω	natural frequency
Ω	rotational frequency
Ω_N	nominal rotational frequency of the WEC (4.59 rad/s)
n	rotor speed (r.p.m.)
θ_0	blade pitch angle
$\theta_{0,\ OPT}$	optimum blade pitch angle for max. power coefficient
$x = r/R$	relative rotor radius
V, V_{WIND}	wind speed
$\lambda = R\Omega/V$	tip speed ratio
$\mu = 1/\lambda$	advance ratio
β	rotor flapping angle
ε	yaw angle, nacelle
y	lateral motion, nacelle
"Δ"	difference symbol
"$\dot{}$"	first derivative w.r.t. time
"$\ddot{}$"	second derivative w.r.t. time

1. Introduction

The wind energy converter (WEC) "MONOPTEROS" (greek: mono-wing) is a 1:3 model scale test version of a single-bladed 5.4 MW horizontal-axis wind turbine. It was developed by Messerschmitt-Bölkow-Blohm Corp., Munich, Germany under contract to the Ministry of Research and Technology of the Federal Republic of Germany (Project GROWIAN II). Since August 1982, the WEC has been connected to the grid of the Bremerhaven electricity system, still undergoing a test phase, and is delivering the designed electrical power of 370 kW.
A hardware impression of the WEC is given in figure 1.

Figure 1: Wind energy converter "MONOPTEROS"

A specification with the basic data is shown in figure 2.

Rotor:

Type	One Blade See-Saw, Downwind
Diameter, m	48
Operational speed, rpm	39 – 48
Design tip speed ratio, $R\Omega/V$	12
Pitch control range, deg	12 – 70
Operational flapping angles, deg	3 – 10

Blade:

Length, m	23
Construction	All composite shell with supporting foam
Solidity	0.018
Aspect ratio	18
Twist (non-linear), deg	14.8
root/tip chord, m	2.33/0.56
Airfoils	Wortmann FX 77 W

Tower:

Type	Steel shell, 3 guy-wires
Diameter, m	1.7
Hub height, m	50

Generator System:

Type	Synchronous AC/Static Freq. Converter
Rating, KVA	454
Speed range, rpm	200 – 1800

Control System:

Pitch/yaw control	electromechanical
Active Power	rotor speed–controlled

Performance:

Rated electr. power, kW	370
Wind speed at hub height, m/s	
• cut in	6
• rated	10
• cut out	16
• survival	50
Annual energy production, Mill kWh	1.3

Figure 2: Specification

The dynamic concept of the WEC "MONOPTEROS" was determined by the requirements of deliberately admitting motions (i.e. oscillations) in order to lower compulsive forces and loads during operation. These requirements are met by the following features of the WEC:

- supercritical performance with a rotor speed, which is above the first tower bending natural frequency (66 % Ω_N),
- flapping degree of freedom (D.O.F.) of the rotor, provided by the gimbaled suspension, within a range of 11.5 deg during operation
- active power control with variable rotor speed.

By reason of the supercritical performance, the system is insensitive w.r.t. the aerodynamic unbalance of the one-bladed rotor and to overspeed. The flapping hinge prevents the introduction of aerodynamic moments, caused by the parasitic thrust, into the hub structure. Furthermore, the gimbaled suspension dynamically decouples almost completely the asymmetric rotor from the tower-nacelle-system. 2/rev-vibrations and possible "Whirl-Flutter"-instabilities, which are induced by fixed system oscillations and the major moment of inertia of the rotor in the case of a rigid hub, do not exist.

The syncronous generator with its frequency converter, as well as the revolution synchronous time rate of the digital active power controls, permit the rotor to perform 1/rev. speed variations, which prevent the transmission of coriolis torque modulations into the shaft and the gearbox.

Figure 3 shows a survey of the first important natural frequencies for the rotor and the tower-nacelle-system as functions of the rotational frequency of the rotor.

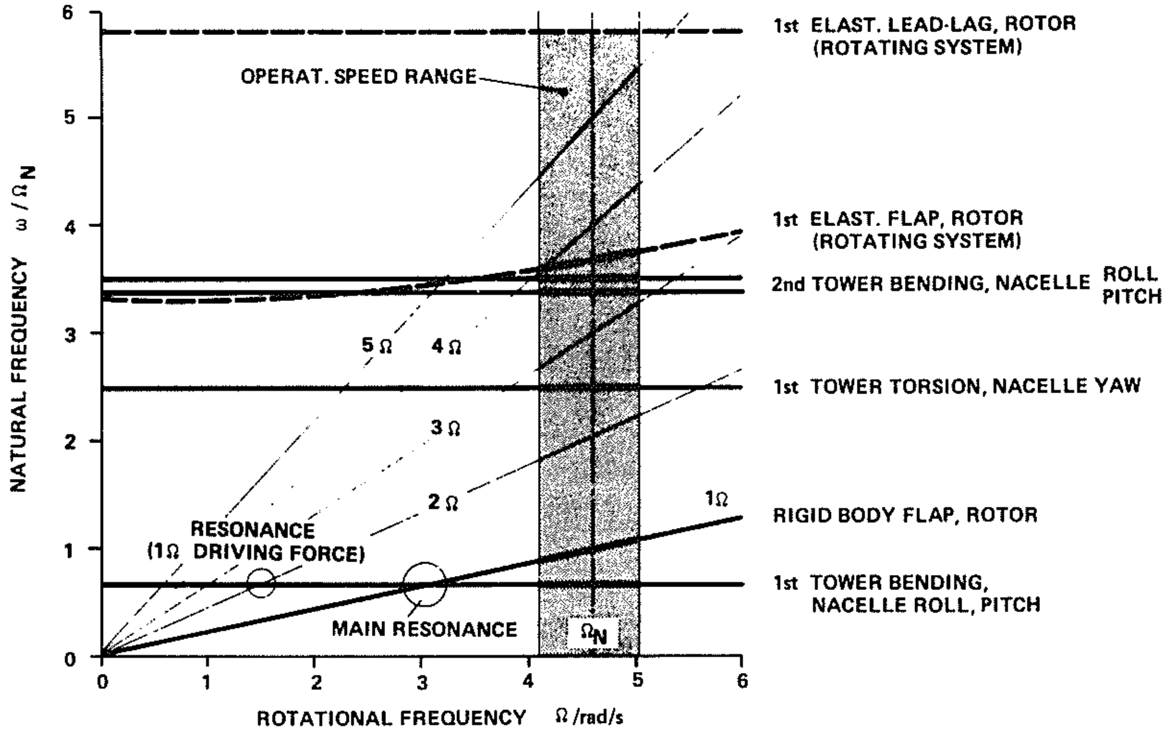

Figure 3: First important rotor-, tower natural frequencies

The arrangement of the components' natural frequencies in the operational speed range guarantees an uncomplicated nominal performance.

The most problematic operating phases of the WEC "MONOPTEROS" are the transients, i.e. the aerodynamic acceleration and the shut-down of the one-bladed rotor. As shown in figure 3, the rotor has to pass the resonances of the first tower bending eigenfrequency. Furthermore, the teetering motion of the rotor is extremely sensitive w.r.t. gusts and control errors during the transients at low rotor r.p.m.,owing to an insufficient centrifugal restoring moment and the lack of aerodynamic flap damping at the counterweight side. The danger of heavy impacts on the dampers, which are delimiting the free flapping motion of the rotor, is obvious. In section 4 efficient blade pitch control strategies, in order to provide a safe passage of tower bending resonances, are presented.

2. Control and Normal Performance Modes

The control and the normal performance modes of the WEC are described by the power-rotor speed diagram in Fig. 4.

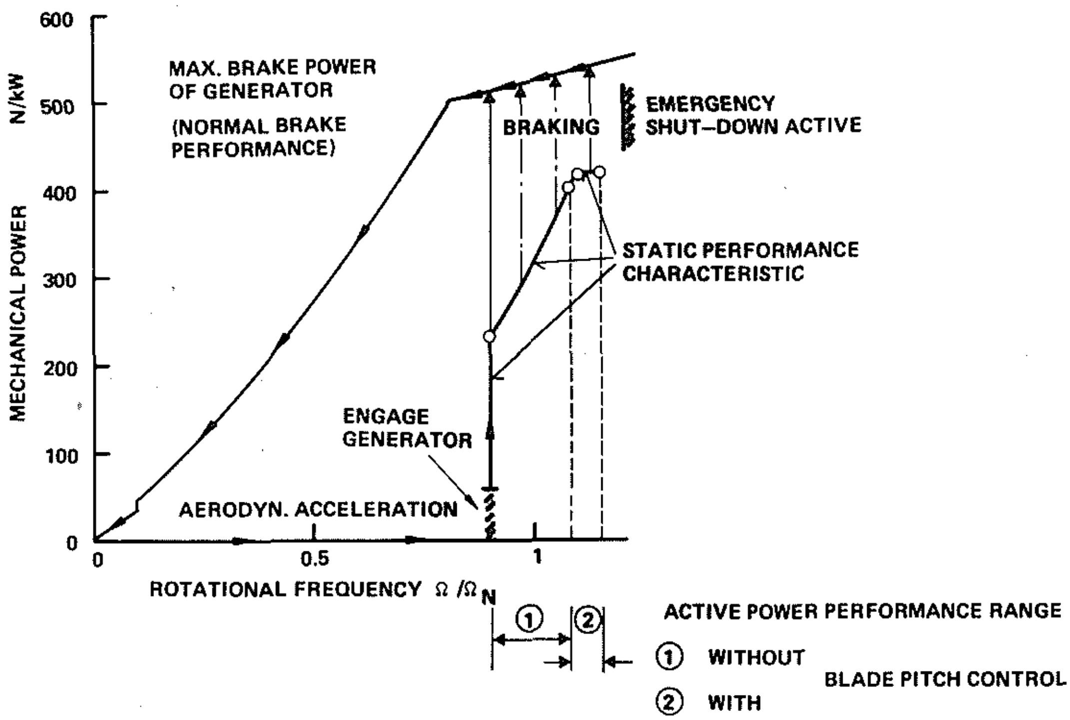

Figure 4: Power characteristics for normal performance modes

The rotor is aerodynamically accelerated by successive adjustment of blade pitch (see section 4). At 90 % nominal rotor speed the generator is engaged. According to the prevailing wind speed the following control ranges have to be distinguished on the static performance characteristic:

a) Wind speed range: 6 m/s < V_{WIND} < 8 m/s :

Performance with constant rotor speed (90 % Ω_N) without blade pitch adjustment at slightly suboptimal blade pitch setting

b) Wind speed range: 8 m/s < V_{WIND} < 10 m/s :

Performance with variable rotor speed from 90 % Ω_N to 108 % Ω_N with optimum blade pitch setting ($\theta_{0,OPT}$) along the cubic power-rotor speed characteristic.

c) Wind speed range: 10 m/s < V_{WIND} < 16 m/s :

Performance with variable rotor speed up to 115 % Ω_N. In this range, the blade pitch control is active for the aerodynamic power limitation and adjusts airfoils in nose-down direction.

The normal shut-down in the automatic-mode performance takes place in the following cases:

a) weak winds, i.e. rotor speed less than 75 % Ω_N

b) strong winds (V_{WIND} ~ 16 m/s); blade pitch control reaches a defined pitch angle limit, when adjusting airfoils nose-down.

During normal shut-down the generator operates along the max. brake power characteristic until 10 % Ω_N. Then the mechanical friction brake is applied. Furthermore, during the braking procedure, the blade is driven into wind vane direction controlled by the flapping angle of the rotor (see chapter 4).

The block diagram of controls of the WEC is shown in Fig. 5. The control system consists of the following circuits:

- Active power control circuit with static nonlinear power characteristic and rotor speed control.
- Blade pitch control circuit with off-normal check in the feedback.
- Circuit for the yaw control of the nacelle for relative zero wind direction adjustment.
- Acceleration and brake control

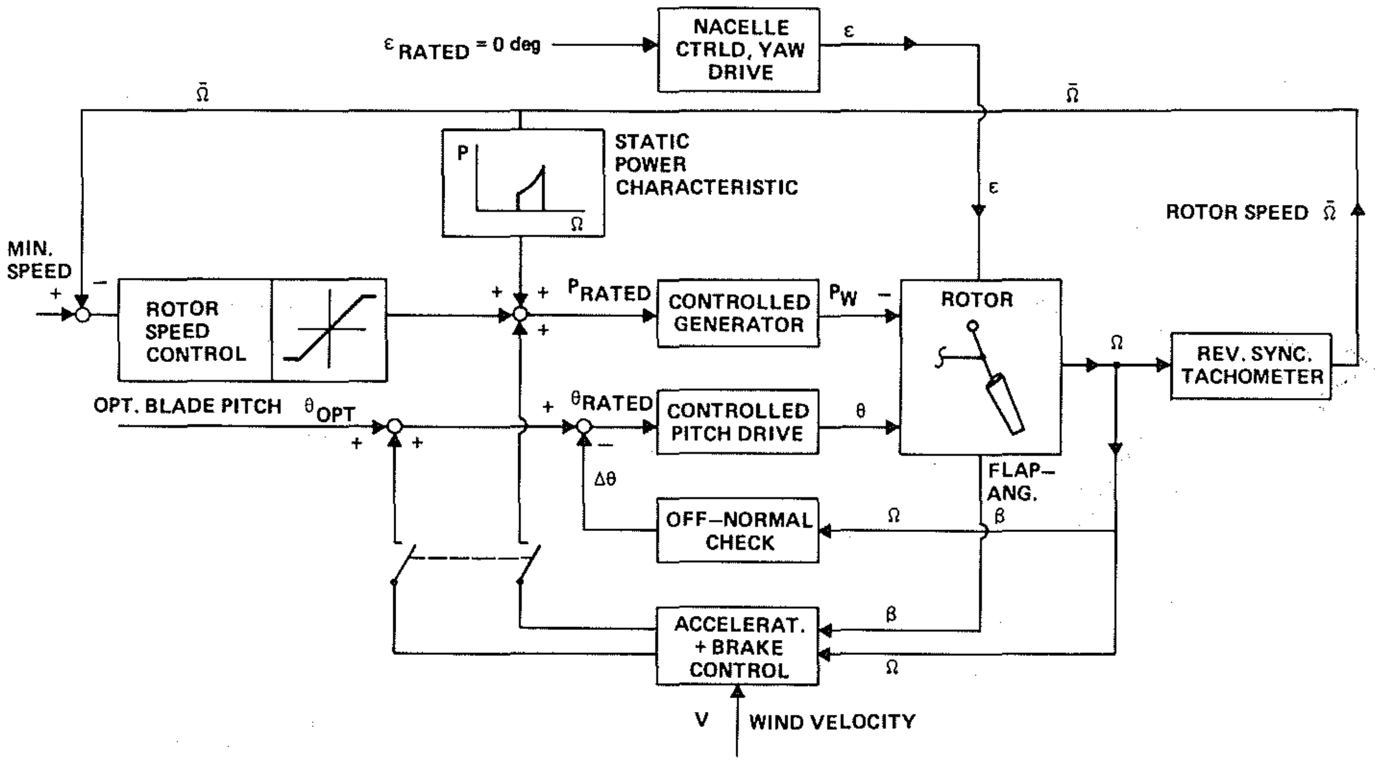

Figure 5: Block diagram of controls

3. Mathematical Modelling

A simple rigid body model in the D.O.F: rotor rotation, rotor flapping, nacelle lateral motion, corresponding to the first tower bending mode has been developed for the prediction of the transient behaviour of the WEC (see Fig. 6).

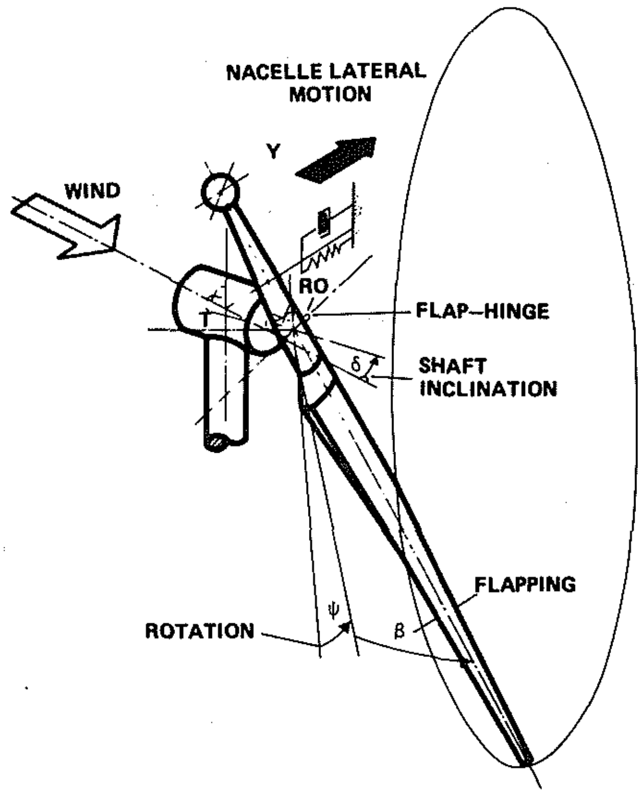

AERODYNAMICS
- BLADE ELEMENT THEORY
- NONLINEAR LIFT, DRAG, PITCH COEFF.
- LOCAL VARIABLE DOWNWASH
- DOWNWASH FOR WINDMILL BRAKE STATE (GLAUERT)
- TIP–LOSS FACTORS (WEINIG, PRANDTL)

DYNAMICS
- ROTOR: ISOLATED, RIGID, (DOF: ROTATION, FLAP)
- *NACELLE: LATERAL MOTION (1st TOWER BENDING)*
- CONTROLS OF OPERATING SYSTEM
- NONLINEAR FLAP DAMPERS

WIND REGIME
- EXP. & LIN. VERTICAL VELOC. PROFILES
- WIND DIRECTION SHEAR
- WIND DIRECTION & NACELLE YAW
- TURBULENT TOWER WAKE
- DETERMINISTIC COHERENT GUSTS

APPLIED NUMERICAL METHODS
- INTEGRAT. ACC. TO RUNGE–KUTTA (4th. O.)
- RECURRENCE OF DIGITAL CONTROL EQUATIONS

RESULTS, PREDICTIONS
- MOTIONS, POWER, LOADS
- SYSTEM BEHAVIOUR IN NORMAL AND OFF–NORMAL PERFORMANCE

Figure 6: Features of the simulation program for transient behaviour prediction

More emphasis has been put upon precise aerodynamic modelling. In order to predict cyclic and higher harmonic excitations for structural analysis, detailed models for the incident flow of the rotor, owing to the surface boundary layer, wind direction and turbulent tower wake [Ref. 1, 2] as shown in Fig. 7, were implemented in the simulation program.

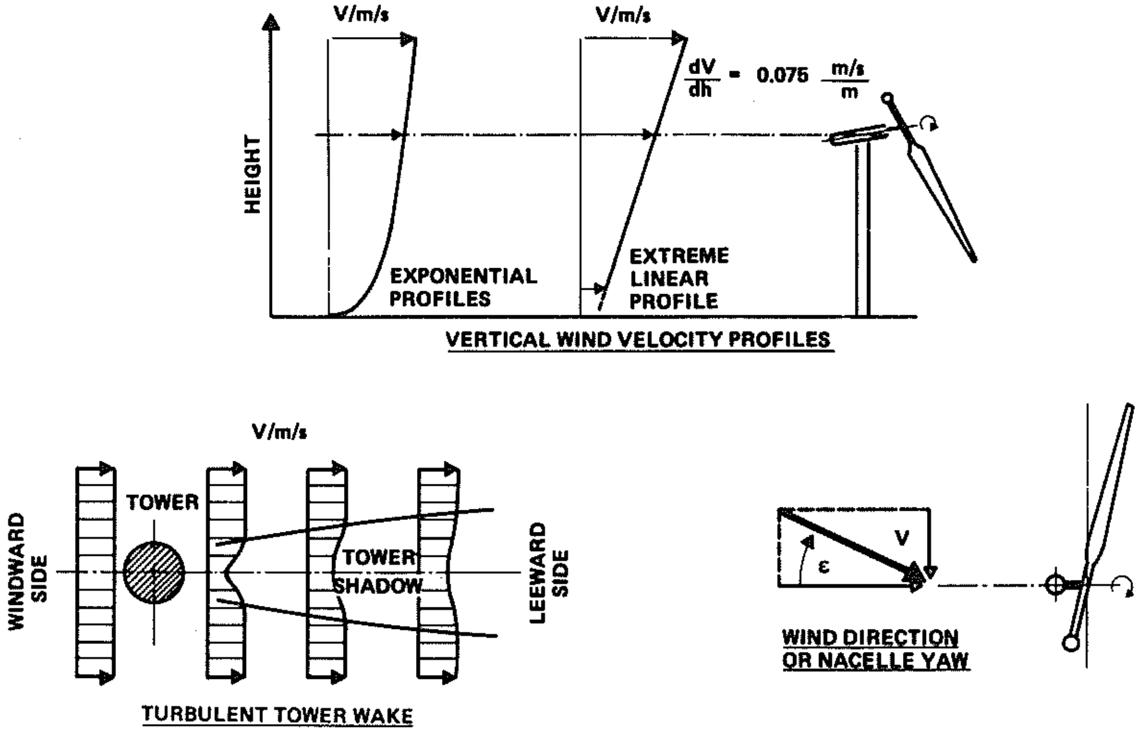

Figure 7: Optional models of incident rotor flow in the simulation program

The modelling of rotor aerodynamics applies the classical approach of blade element theory, measured airfoil data, momentum law and tip-loss factors [Ref. 3].
The validity of Prandtl's tip-loss factor

$$F_P = \frac{2}{\pi} \text{ arc cos } e^{-f} \qquad \text{with } f = \frac{B}{2} \frac{1 - x}{\sin \phi}$$

B ≙ number of blades; ϕ ≙ inflow angle
$x = r/R$ ≙ relative rotor radius

is problematic in the case of a one-bladed rotor especially at low rotor speed (i.e. high advance ratio $\mu = V/R\Omega$ in classical propeller theory, small tip speed ratio $\lambda = R\Omega/V$ in windmill theory).

For this reason a tip-loss factor according to Weinig [Ref. 4]

$$F_W = \frac{1 + 2x}{4\pi} \sqrt{\frac{1 - x}{x^3}}$$

is applied in the tip speed ratio range $0 \leqq \lambda \leqq 2$. This factor correctly shapes the thrust distribution in the case of a one-bladed rotor with optimum circulation distribution at high advance ratios ($\mu = V/R\Omega$).

By reason of achieving a most exact description of the control system, the original recursive digital filters, which are implemented in the real time control program of the WEC, were applied. Furthermore, a simplified performance mode selection logic was used in order to simulate the automatic generator engagement or shut-down under defined conditions.

Additionally, the hydraulic nonlinear damping system which delimits the free flapping motion of the rotor ($+2 \text{ deg} \leqq \beta \leqq 13.5 \text{ deg}$), has been modelled according to the hardware specifications.

4. Development of Control Strategies for Rotor Acceleration and Shut-Down

4.1 Aerodynamic Acceleration

The aerodynamic acceleration of the WEC "MONOPTEROS" is rendered by the blade pitch drive within an angular range from $\theta_0 = -100°$ (airfoils at 60 % blade radius nearly in wind vane position) up to $\theta_0 = -7°$ (airfoils positioned nearly parallel with rotor disc area). The starting procedure of the WEC has the following sequence:
After having averaged the wind speed signal, measured on the nacelle roof, over a period of 90 s, the control system feeds the mean value into the control function for the blade pitch adjustment. Then the rotor is unlocked and the blade pitch angle follows the increasing rotor speed as shown by the heavy drawn curve in the θ_0-λ-diagram of figure 8.

From the well-known velocity diagram at a blade element (see Fig. 8, top right) an approximate dependence between the blade pitch angle θ_0 and the rotational frequency Ω of the rotor as well as the wind speed V can be derived (see Fig. 8, left diagram, dashed curve). According to the formula given above in Fig. 8, θ_0 is varied in such a manner that a chosen value for the angle-of-attack (α_{DESIGN}) is held constant at a blade section x, where the average resultant driving force is expected during acceleration. According to the lift coefficient (c_L) vs. angle-of-attack in Fig. 8 (bottom left) it is obvious that the determination of α_{DESIGN} was the subject of intensive simulation studies. In the case of having chosen α_{DESIGN} too small, the rotor does not accelerate, or, worse, the rotor speed can stick before the main resonance frequency of the tower. If the angle-of-attack is chosen for achieving maximum lift (C_{LMAX}), the rotor runs the risk of a stall-induced flap instability. These two extreme design points for the control law seem very sensitive w.r.t. neglected dynamic velocity components originating from the blade flapping motion, changes in wind speed and induced velocity. The deviation of the control function of the tip speed ratio $0 \leqq \lambda \leqq 3$ originates from the limited blade pitch drive speed of max. 8.5 deg/s.

In order to "capture" the rotor during generator engagement without running the risk of overspeed, the blade pitch angle is already held constant at 50 % nominal rotor speed.

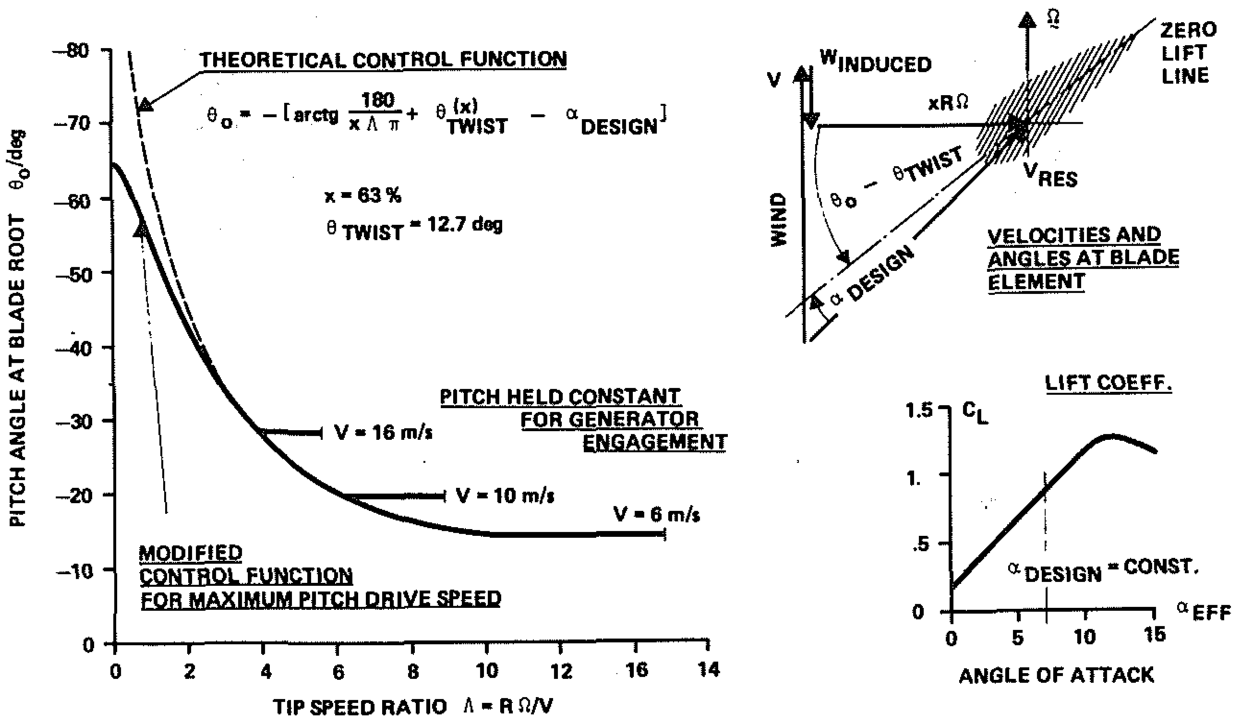

$$\theta_o = -[\text{arctg}\,\frac{180}{x\Lambda\pi} + \theta_{TWIST}^{(x)} - \alpha_{DESIGN}]$$

Figure 8: Blade pitch control function for aerodynamic rotor acceleration

The quasi-static developments of the driving force and thrust distribution at the blade during an accleration, at a wind speed of 10 m/s, until generator engagement are shown in Figs. 9 and 10.

Owing to the modified control function, the rotor aerodynamically starts in post-stall (see driving force distributions tions in Figure 9, range $0 \leq \lambda \leq 1.5$ for outer blade parts $x < 60$ %). The driving force distributions at tip speed ratios $6 < \lambda < 9$ (before the generator engagement) are slightly suboptimal (optimum shape: elliptic) due to the fact that the estimated origin ($x = 63$ %) of the resultant driving force is assumed to be locally constant in the control law.
The development of the thrust distribution in Figure 10 shows the change in the aerodynamic state from the fixed wing to the typical rotor-like distribution.

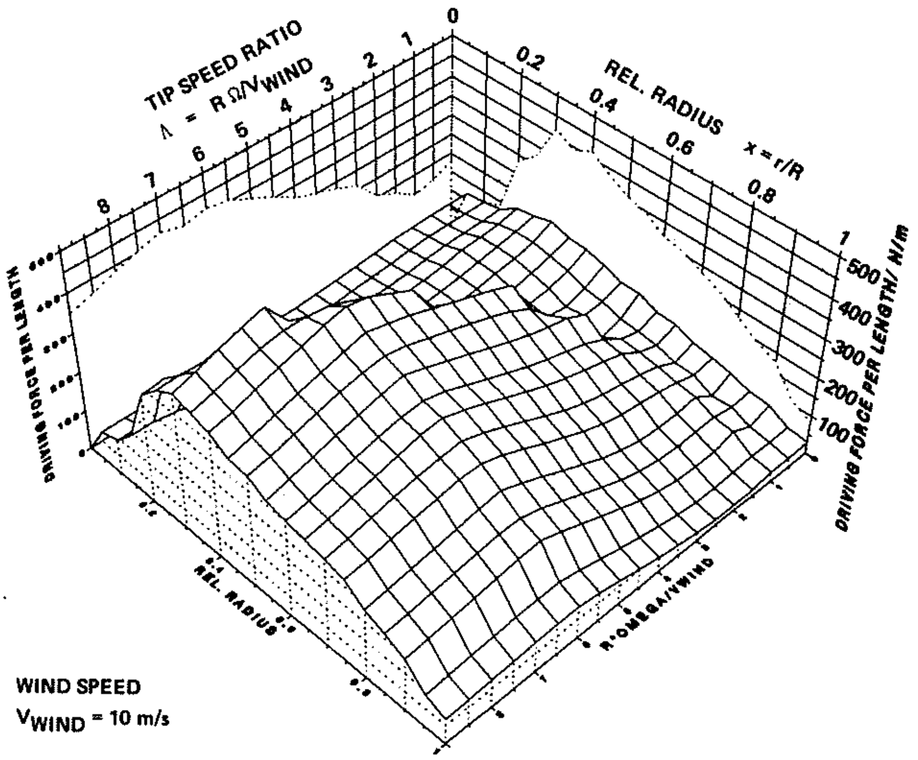

Figure 9: Development of driving force distribution during aerodynamic acceleration

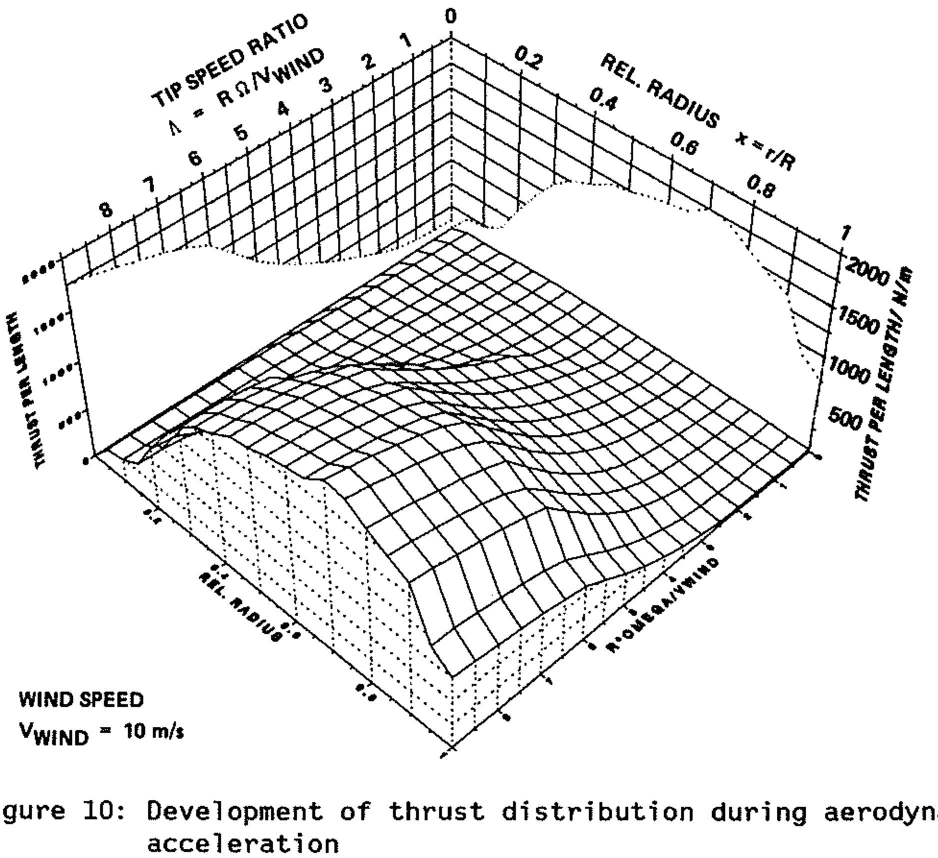

Figure 10: Development of thrust distribution during aerodynamic acceleration

4.2 Shut-Down

The one-bladed rotor cannot be braked during the power-limited performance with operational blade pitch setting. With decreasing rotor speed and constant blade pitch angle, the rotor would always climb over a maximum of the aerodynamic flapping moment characteristic and dangerously impact the flap dampers in a state of high rotational energy. To avoid this effect, the blade pitch angle is adjusted into wind vane direction by hysteresis control, dependent on defined limits of the flapping angle as shown in Fig. 11.

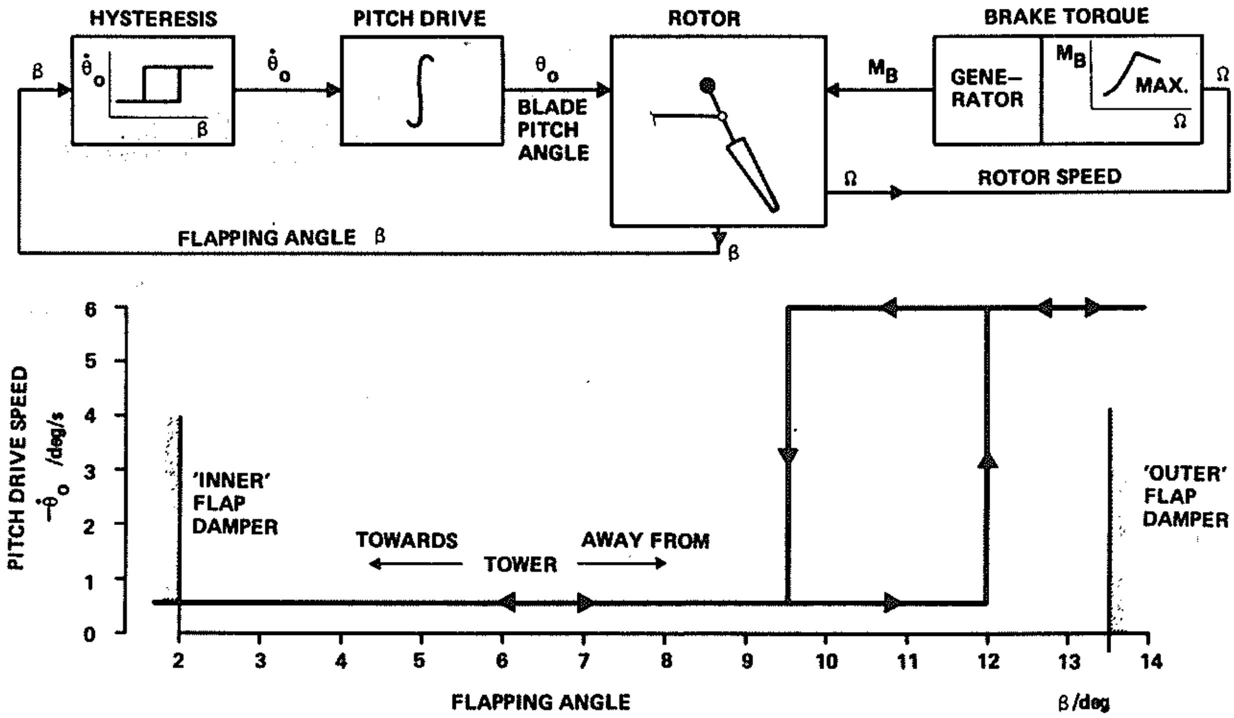

Figure 11: Command procedures for normal shut-down

5. Transient Behaviour of the WEC "MONOPTEROS"

5.1 Acceleration into Nominal Performance

Figure 12 shows a simulation of an acceleration into nominal performance, carried out with a computer program according to the model discussed in section 3. The rotor operates under deterministic wind regime data, i.e. constant wind speed, exponential vertical wind velocity profile and without tower wake influence, which is only interesting in the case of load prediction. The control function shown in Fig. 8 is valid in the time interval $0 \leq t \leq 33$ s.
Then the performance mode is changed and the operational control leads the system into nominal performance without overshooting the rotor speed.

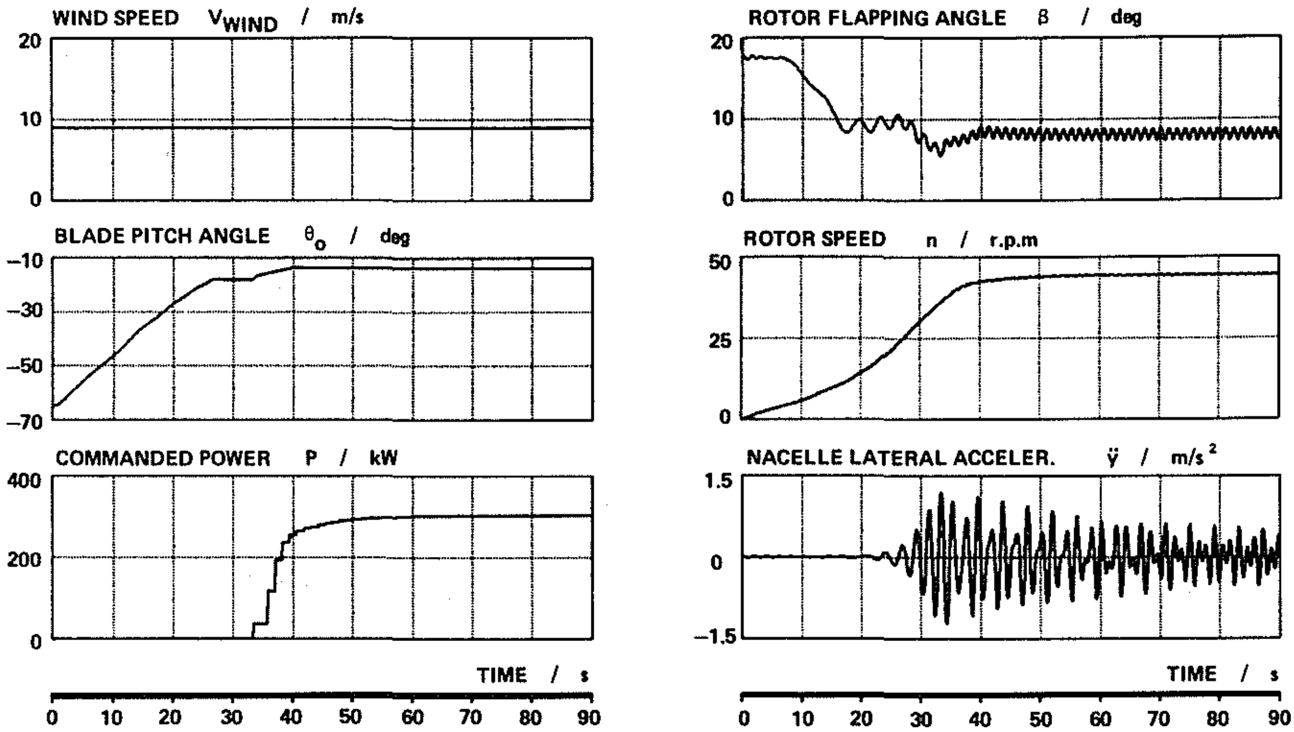

Figure 12: Acceleration at wind speed V = 9 m/s (simulation)

At low r.p.m. the rotor is in contact with the "outer" flap delimiter and is driven into operational angular range with increasing rotor speed by the centrifugal flapping moment. The 1/rev-modulation of the flapping angle in the simulation shown originates from the exponential vertical wind velocity profile (see Fig. 7) and the rotor shaft inclination of 9 degs.

A comparable measurement of an acceleration is given in Figure 13. Here the flapping angle shows greater modulations in steady state by reason of wind direction influence which was neglected in the simulation. The acceleration starts at the time t = 8 s and shows good correlation with the simulation w.r.t. duration as well as to the shape of input and response channels. A good correlation between measurement and theory is also obtained in the lateral accleration $\ddot{y}$ of the nacelle concerning the peak values of the main tower bending resonance (28.9 r.p.m.). The slow decay of amplitudes is due to the small structural damping (1 % crit.) of the steel tower.

5.2 Gust Response

Figure 14 shows a measured gust response of the WEC, when operating near the active power limitation. For this test run of the WEC, the limit of power command in the control program has been set at 400 kW instead of the specified value of 370 kW.

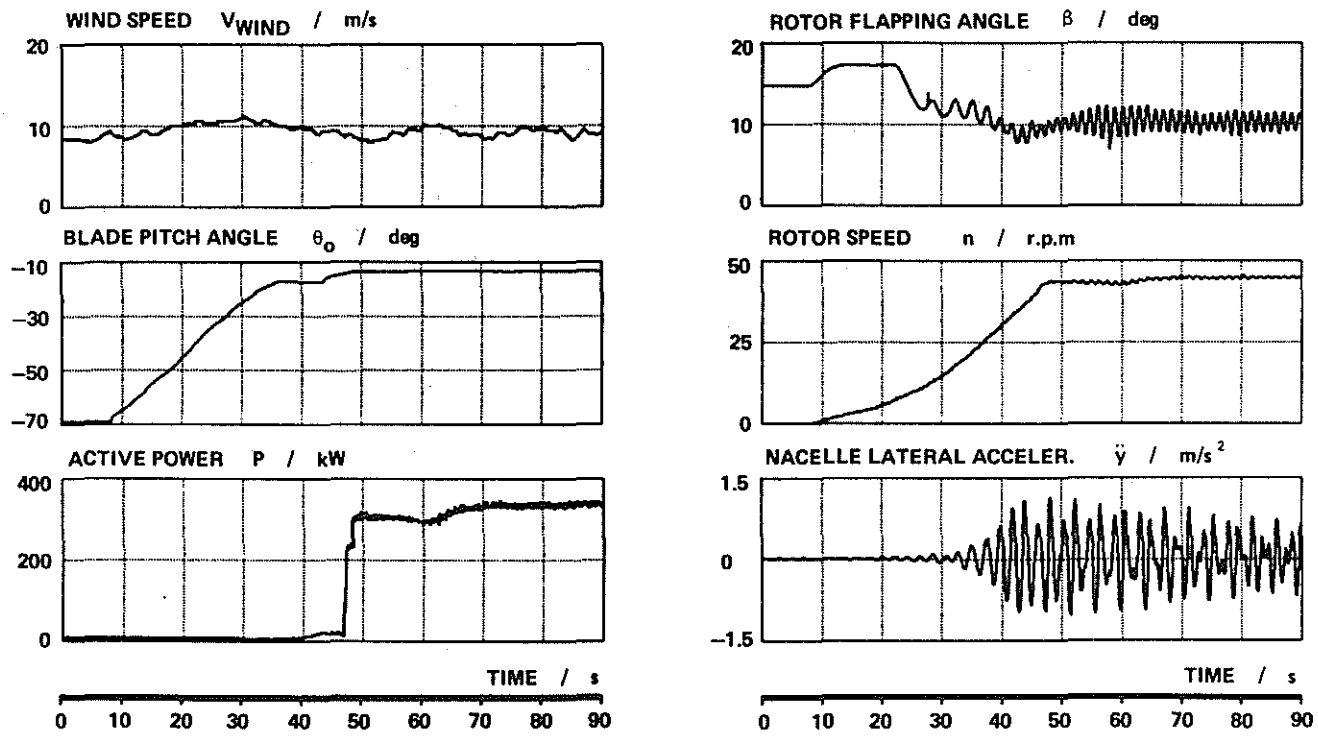

Figure 13: Acceleration at mean measured wind speed V = 9 m/s (measurement)

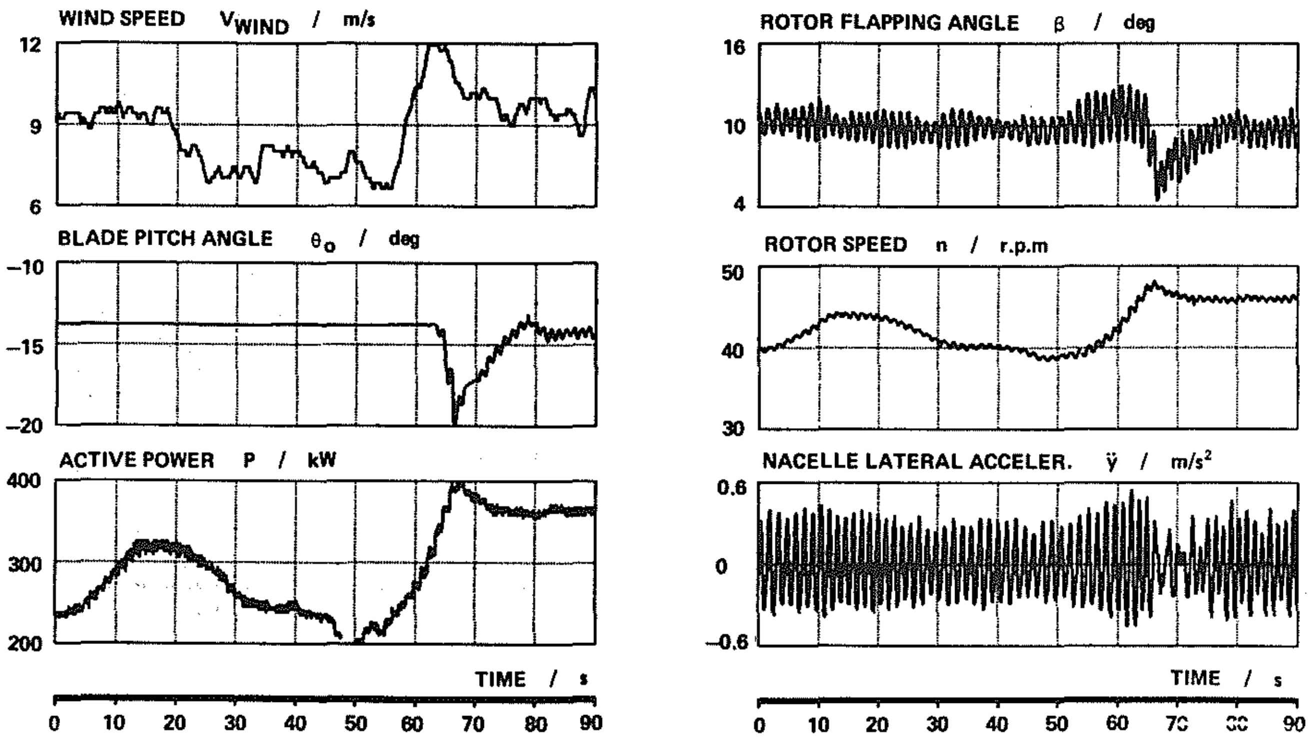

Figure 14: Gust response (measurement)

As already discussed in section 2, the rotor is only speed-controlled for wind speeds below 10 m/s. This can be observed in the time interval $0 < t < 62$ s. Owing to the first gust, rising before the time window shown in Fig. 14, the WEC varies rotor speed and active power, but not the blade pitch angle. The mean value of the blade pitch angle is then relatively insensitive w.r.t. the resulting fluctuation in centrifugal flapping moment. Flapping behaviour distinctly changes when the blade pitch control is active (second gust, rising at $t = 56$ s). In the measurement shown, the blade is flapping towards the tower when the blade pitch drive turns the airfoils in nose-down direction. The flap sensitivity w.r.t. the blade pitch angle adjustment, as can be read from the time histories, is 1 deg flap per 1 deg pitch in this performance state (considering only mean variations).

5.3 Normal Shut-Down

A normal shut-down at high windspeed is shown in Fig. 15 (see time $t = 39$ s).

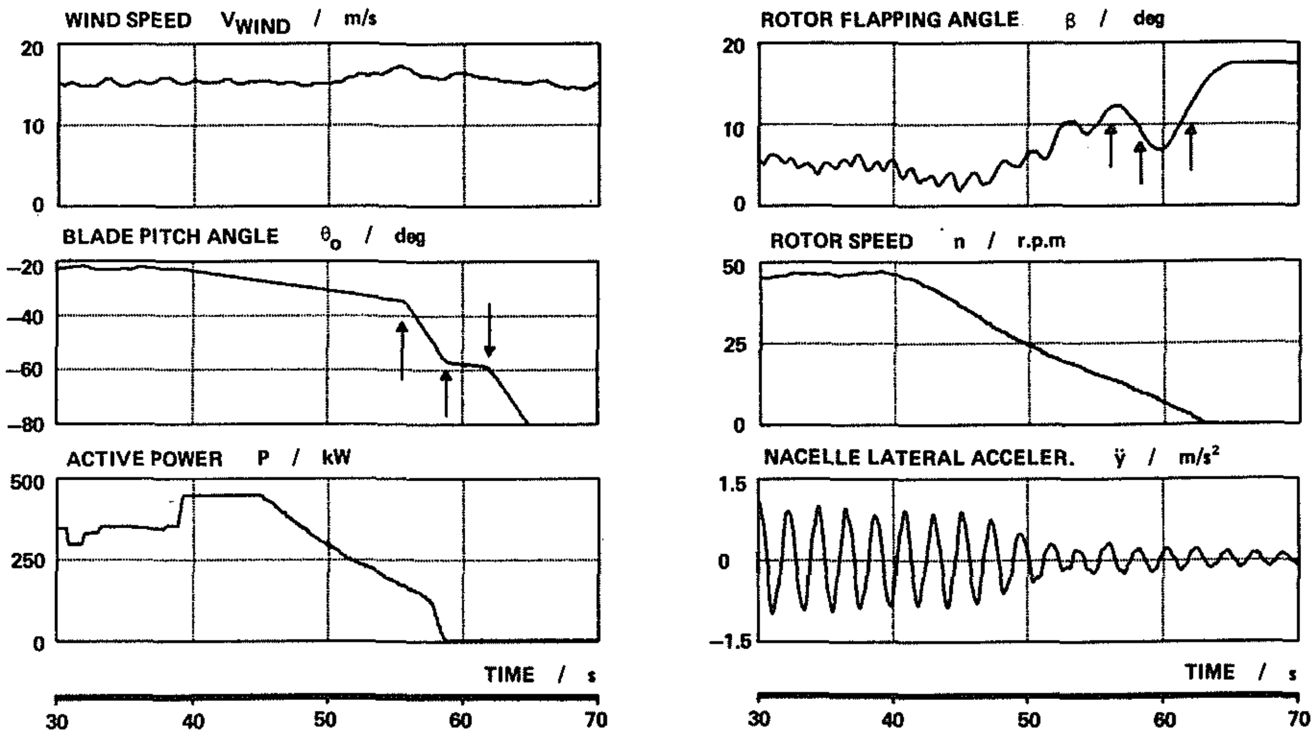

Figure 15: Normal shut-down at high wind speed (measurement)

The blade pitch angle is controlled analoguously to the hysteris shown in figure 11 depending on the flapping angle. The generator brakes the rotor according to the time history of active power shown (see also figures 4 and 11).

In the time interval 40 s < t < 50 s the rotor is slightly in contact with the "inner" flap dampers, delimiting the flapping motion towards the tower. At the end of the shut-down the rotor smoothly flaps into the opposite limitation (see t > 62 s).

6. Conclusions

The transitions of a one-bladed, supercritically operating, horizontal-axis wind-turbine can be coped with by efficient strategies for computer control. The corresponding parameters can only be tailored by simulation. Therefore the establishment of a model with the following features is sufficient:

- simple rigid body dynamics of the rotor and tower-nacelle-system concerning critical D.O.F.
- classical, stationary rotor aerodynamics, but with special regard to the tip-losses at low rotor speed
- almost exact description of the control system

7. References

1) W. Frost, et al., Engineering Handbook on the Atmospheric Environmental Guidelines for Use in Wind Turbine Generator Development NASA, Technical Paper 1359, 1978

2) H. Pfeil, et al., Messungen im turbulenten Nachlauf des Einzelzylinders, Verein Deutscher Ingenieure (VDI), Forschung Ingenieur-Wesen, Vol. 41, Nr. 5, 1975

3) R.E. Wilson, et al., Aerodynamic Performance of Wind-Turbines, Oregon State University, Corvallis, USA, June 1976 (National Science Foundation Report RA-760228)

4) F. Weinig, Aerodynamik der Luftschraube, Julius Springer, Berlin 1940